J Mater Sci: Mater Med (2011) 22:607–615
DOI 10.1007/s10856-011-4228-4

Preparation and preliminary cytocompatibility of magnesium doped apatite cement with degradability for bone regeneration

Jingxiong Lu · Jie Wei · Yonggang Yan · Hong Li · Junfeng Jia · Shicheng Wei · Han Guo · Tiqiao Xiao · Changsheng Liu

Received: 24 October 2010 / Accepted: 3 January 2011 / Published online: 22 January 2011

Abstract In the present study, we fabricated magnesium doped apatite cement (md-AC) with rapid self-setting characteristic by adding the mixed powders of magnesium oxide and calcium dihydrogen phosphate (MO–CDP) into hydroxyapatite cement (HAC). The results revealed that the md-AC with 50 wt% MO–CDP could set within 6 min and the compression strength could reach 51 MPa after setting for 1 h, indicating that the md-AC had highly initial mechanical strength. The degradability of the md-AC in Tris–HCl solution increased with the increase of MO–CDP amount, and the weight loss ratio of md-AC with 50 wt% MO–CDP was 57.5 wt% after soaked for 12 weeks. Newly flake-like apatite could be deposited on the md-AC surfaces after soaked in simulated body fluid (SBF) for 7 days. Cell proliferation ratio of MG_{63} cells on md-AC was obviously higher than that of HAC on days 4 and 7. The cells with normal phenotype spread well on the md-AC surfaces and attached intimately with the substrate, and alkaline phosphatase (ALP) activity of the cells on md-AC significantly improved compared with HAC on day 7. The results demonstrate that the md-AC has a good ability to support cell proliferation and differentiation, and indicate a good cytocompatibility.

J. Lu · J. Wei (✉) · J. Jia · C. Liu (✉)
Key Laboratory for Ultrafine Materials of Ministry of Education, State Key Laboratory of Bioreactor Engineering, East China University of Science and Technology, Shanghai 200237, China
e-mail: jiewei7860@sina.com

C. Liu
e-mail: biomater2006@yahoo.com.cn

J. Lu
e-mail: jingxionglu@yahoo.cn

Y. Yan · H. Li
School of Physical Science and Technology, Sichuan University, Chengdu 610064, China

S. Wei
Center for Biomedical Materials and Tissue Engineering, Academy for Advanced InterDisciplinary Studies, Peking University, Beijing 100871, China

H. Guo · T. Xiao
Shanghai Synchrotron Radiation Facility, Shanghai Institute of Applied Physics, Chinese Academy of Sciences, Shanghai 201800, China

1 Introduction

In 1986 Brown and Chow firstly reported hydroxyapatite cement (HAC) with excellent biocompatibility and osteoconductivity [1]. A typical self-setting HAC contains an equimolar mixture of tetracalcium phosphate (TECP, $Ca_4(PO_4)_2O$) and dicalcium phosphate anhydrous (DCPA, $CaHPO_4$). It can harden within 30 min after the powder is mixed with water to form a paste that changes into hydroxyapatite (HA, $Ca_{10}(PO_4)_6(OH)_2$) as the final product. This process is based on an acid-basic neutralization reaction as follows:

$$2Ca_4(PO_4)_2O + 2CaHPO_4 \rightarrow Ca_{10}(PO_4)_6(OH)_2$$

The TECP/DCPA system apatite bone cement has unique properties in vivo: slow resorption and replacement by new bone tissue [2, 3]. However, a rapid replacement by new bone is desirable in some clinical situations.

Previous studies show that magnesium (Mg) indirectly influences mineral metabolism of bone. For example, through activation of alkaline phosphatase, the attachment and spread of cultured human bone derived cells on the Mg-coated Al_2O_3 bioceramic is significantly enhanced compared with the uncoated Al_2O_3 [4, 5]. Mg ion

embedded HA coating on TiAlV significant improves bone bonding property when compared with an ordinary hydroxyapatite coating [6]. In recent years, magnesium alloys have attracted more and more attention as a potential matrix material for biodegradable implants in biomedical application [7–9]. Some studies have showed that Mg is toxic-free, and it is acceptable of Mg ion to gradually enter the human body [5, 7]. Magnesium can increase the solubility of phosphates after Mg substitutes the part of calcium [10, 11]. Brushite cements containing Mg may offer a new way to control microstructure, mechanical strength, composition and resorbability of the biocement [12].

Calcium phosphate cements are generally prepared by mixing two or more phosphate salt components of an acid phosphate and a basic calcium salt (or phosphate) with an aqueous solution. These cements can self setting and present appropriate mechanical properties due to an acid-basic neutralization reaction. Our previously prepared magnesium phosphate cement (MPC) consisted of magnesium oxide (MgO) and ammonium dihydrogen phosphate ($NH_4H_2PO_4$) for biomedical applications, which had a good biocompatibility after implanted into cavities in the femoral condyle of rabbits [13, 14]. Wu et al. studied calcium-magnesium phosphate cement (CMPC) by incorporation of MPC into CPC [15]. Jie et al. prepared hierarchical microporous/macroporous scaffold of magnesium-calcium phosphate for bone tissue regeneration [16]. However, the final product of magnesium ammonium phosphate hexahydrate [$NH_4MgPO_4 \cdot 6H_2O$] containing NH_4 group would release NH_3 in the physiological environment and generate some effects on cytocompatibility. In this study, we prepared magnesium doped apatite cement (md-AC) by adding a mixture of magnesium oxide and calcium dihydrogen phosphate (MO–CDP) into TECP/DCPA system apatite cement.

2 Materials and methods

2.1 Preparation of md-AC powders

The magnesium doped apatite cement (md-AC) powders were prepared by adding MO–CDP powders into HAC with different weight ratios as shown in Table 1. The MO–CDP cement powders consisted of magnesium oxide (MgO) and calcium dihydrogen phosphate ($Ca(H_2PO_4)_2 \cdot H_2O$) in a molar ratio of 7:3, which was designed to generate magnesium substitute calcium apatite (md-CA, $(Mg_7Ca_3)(PO_4)_6(OH)_2$) cement according to the acid-basic neutralization reaction as follows:

$$7MgO + 3Ca(H_2PO_4)_2 \rightarrow (Mg_7Ca_3)(PO_4)_6(OH)_2 + 5H_2O$$

MgO was prepared by heating magnesium carbonate pentahydrate in a furnace at 1500°C for 6 h. The resultant powder was cooled to room temperature, and then grounded in a planetary ball mill for 3 min, followed by sieving through 200 meshes for further use.

The HAC powders consist of TECP and DCPA in an equal molar ratio, and the preparation method was as previously described [3]. Briefly, TECP was synthesized by a solid-to-solid reaction between calcium phosphate and calcium carbonate at a temperature of 1500°C for 8 h. Dicalcium phosphate dehydrate (DCPD) was prepared from ammonium hydrogen phosphate and calcium nitrate in the acidic environment. DCPA was obtained by removing the crystallization water in DCPD at 120°C for 5 h. All the chemicals used were purchased from Sinopham Chemical Reagent Co., Ltd. Shanghai, China.

2.2 Characterization of md-AC

The md-AC paste was formed by mixing md-AC powders with water. The setting time of md-AC (HAC as a control) was determined by a Vicat apparatus bearing a 300 g needle 1 mm in diameter. The setting time was determined as the number of minutes elapsed from the start of the mixture to the time when the needle failed to make a 1 mm deep circle on the surface of the specimen in the environment of 37°C and 100% humidity. The average value for at least three tests was calculated for each specimen, and the results were expressed as mean ± standard deviation (M ± SD). As controls, the MO–CDP cement samples were prepared under the same experimental conditions.

Pre-hardened md-AC (HAC as a control) samples for the compression strength test were obtained by putting the pastes into Teflon-molds with the size of Φ 6 × 10 mm in the environment of 37°C and 100% humidity for 48 h. The compression strength was measured with a universal testing machine (AG-2000A, Shimadzu) at a speed of 1 mm/min until failure. Three replicates were carried out for each group, and the results were expressed as M ± SD. The surface morphology/microstructure and composition of the pre-hardened md-AC samples after 48-h setting were characterized by a scanning electron microscope (FE-SEM, Hitachi Ltd, S-4300SE, Japan), X-ray diffraction (XRD; Rigaku Co., Japan). In other experiments, the samples of

Table 1 Effects of MO–CDP amounts on setting time and compressive strength (48 h) of md-AC, data represent the mean ± standard deviation, $n = 3$

MO–CDP (wt%)	Setting time (min)	Compressive strength (MPa)
0 (HAC)	12 ± 0.4	38 ± 2.0
15	9 ± 0.3	49 ± 2.6
30	7 ± 0.2	63 ± 1.8
50	6 ± 0.2	72 ± 2.3

md-AC and HAC with different sizes were prepared by using different mould after 48-h setting under the same conditions.

2.3 Degradation of md-AC

The degradability of the md-AC (HAC as a control) was determined by examining the weight loss ratio of the samples in Tris–HCl solution at different time points. The samples (Φ 10 × 3 mm), with initial weight W_0, were immersed into Tris–HCl solution with a weight-to-volume ratio of 0.2 g/ml in plastic bottles. The plastic bottles were continuously shaken at 100 r/min in a water bath at 37°C. After different time periods, the samples were removed from the Tris–HCl solution, cleaned with deionized water, dried at 60°C for 2–4 h, and the new weight W_t was recorded. The samples were then re-immersed into a fresh Tris–HCl solution at the same weight-to-volume ratio followed by continuous shaking. This process was repeated over a period of 12 weeks for all samples. The weight loss ratio of each sample at different time points was calculated according to the following equation:

$$\text{Weight loss ratio } (\%) = (W_0 - W_t)/W_0 \times 100$$

Three samples of each kind of cement were tested, and the results of average value (M ± SD) were shown.

2.4 Immersion in SBF and ion concentration change

The in vitro bioactivity of md-AC with 50 wt% MO–CDP samples was evaluated by examining the newly formed apatite on their surfaces in SBF. SBF was prepared by dissolving reagent-grade NaCl, $NaHCO_3$, KCl, $K_2HPO_4 \cdot 3H_2O$, $MgCl_2 \cdot 6H_2O$, $CaCl_2$, and Na_2SO_4 in deionized water. The solution was buffered at pH 7.4 with tris(hydroxymethyl) aminomethane ($(CH_2OH)_3CNH_2$) and 1 M hydrochloric acid (HCl) at 37°C. Pre-hardened md-AC samples (Φ 10 × 3 mm) were soaked in 30 ml of SBF at 37°C with shaking and without change the solution during soaking. After soaking for different time periods, the specimens were removed from the SBF solution, gently rinsed with deionized water, and dried at room temperature. The morphology of apatite formation on the md-AC surfaces was characterized by SEM.

At each time point (6, 12, 24, 48, 72, 120 and 168 h), the md-AC samples were taken out, and the ion concentrations of Ca, Mg and P in SBF were measured with an inductively coupled plasma atomic emission spectroscopy (ICP-AES, IRIS 1000, Thermo Elemental, USA). The pH of the SBF solution was determined with an electrolyte-type pH meter at each time point. The values obtained from three samples were averaged (M ± SD).

2.5 Cell proliferation and morphology

Cell proliferation was evaluated by seeding MG_{63} cells with a density of 4×10^4 on the md-AC with 50 wt% MO–CDP and HAC (Φ 10 × 3 mm), followed by incubation for 1, 4 and 7 days, with the medium replaced every 2 days. The cell/sample constructs were placed in culture medium containing MTT and incubated in a humidified atmosphere at 37°C for 4 h. Cell proliferation was determined by a MTT assay (MTT Kit, Roche Diagnosis Corp., IN, USA). The optical density (O.D.) absorbance value was measured at 570 nm with microplate reader. Five specimens were tested for each incubation period, and each test was performed in triplicate (M ± SD). The results were reported as OD.

The morphology of MG_{63} cells cultured on the md-AC with 50 wt% MO–CDP (Φ 10 × 3 mm) was observed by SEM. Approximately 50 μl of culture medium containing 4×10^4 cells was seeded on the samples, which had been previously placed in 24 well culture plates. Cells were allowed to attach to substrates for 4 h, and then 1 ml of fresh culture medium was added to each well. Cells were incubated for 7 days in a humidified atmosphere at 37°C and 5% CO_2. Then the cell/sample constructs were washed twice with PBS solution and fixed with 4% formalin in PBS (pH 7.4) for 30 min. They were subsequently washed twice with PBS and dehydrated in a series of graded ethanol (50, 60, 70, 80, 90 and 100% v/v) for 3 min each. Finally, specimens were air-dried in a desiccator overnight for SEM observation.

2.6 Alkaline phosphatase activity

MG_{63} cells with a density of 4×10^4 were seeded on the md-AC with 50 wt% MO–CDP and HAC (Φ 10 × 3 mm), and ALP activity was measured at on days 4 and 7, respectively. At the end of incubation time, the culture medium in 24-well plates was aspirated. Then, 200 μl of 1% Nonidet P-40 (NP-40) solution was added to each well and incubated for 1 h. The cell lysate was obtained and centrifuged. Then 50 μl supernatant was added to 96-well plates, 50 μl of 2 mg/ml *p*-nitrophenylphosphate (Sangon, Shanghai, China) solution composed of 0.1 mol/l glycine and 1 mmol/l $MgCl_2 \cdot 6H_2O$ was added, and incubated for 30 min at 37°C. The reaction was quenched by adding 100 μl, 0.1 N NaOH, and the absorbance of ALP was quantified at the wavelength of 405 nm using a microplate reader (SPECTRAmax 384, Molecular Devices, USA). The total protein content in cell lysate was determined with the bicinchoninic acid (BCA) method in aliquots of the same samples with the Pierce protein assay kit (Pierce Biotechnology Inc., Rockford, IL), read at 565 nm and calculated

according to a series of albumin (BSA) standards. The ALP levels were normalized to the total protein content. All experiments were performed in quadruple and the results were expressed as M ± SD.

2.7 Statistical analysis

Statistical analysis was conducted using one-way ANOVA with post hoc tests. The results were expressed as M ± SD. A value of $P < 0.05$ was considered to be statistically significant.

3 Results

3.1 Setting time and compression strength

Table 1 shows the effect of the MO–CDP amount on setting time and compression strength of md-AC. The setting time of md-AC decreased with the increase of MO–CDP amount. The optimum setting time was obtained at about 6 min. Compared with HAC, md-AC showed a shorter setting time, indicating that md-AC had a fast setting property. As for compression strength, we found that the compression strength of md-AC increased with the increase of MO–CDP after setting for 48 h. The results revealed that the amounts of MO–CDP in md-AC had significant effects on its compression strength.

Table 2 shows the effects of setting time on compression strength of md-AC with 50 wt% MO–CDP. The initial compression strength of md-AC could reach 51 MPa after setting for 1 h while that of HAC was only 13 MPa, and then the compression strength of md-AC slightly increased with time. After 2 days of setting, the compression strength of md-AC could retain as high as 72 MPa while that of HAC was only 38 MPa. The results indicated that the md-AC had much higher compression strength than HAC.

Table 2 Effects of setting time on compressive strength of md-AC with 50 wt% MO–CDP, data represent the mean ± standard deviation, $n = 3$

Time (h)	Compressive strength (MPa)	
	md-AC	HAC
1	51 ± 2.0	13 ± 1.6
6	55 ± 1.4	17 ± 1.8
12	61 ± 1.8	23 ± 1.5
24	67 ± 2.0	31 ± 1.8
48	72 ± 2.3	38 ± 2.2

3.2 Morphology and microstructure

Figure 1 shows the SEM images of surface morphology/microstructure of md-AC with 50 wt% MO–CDP and HAC after setting for 2 days. We observed some obvious difference of surface morphology/microstructure between md-AC and HAC. The md-AC included crystal-like small grains that closely combined with each other; while HAC contained clay-like nubbly substances that formed a microporous structure. The results suggested that the md-AC could be changed into a mixture of apatite crystals by a hydrated reaction.

3.3 XRD analysis

The phase compositions of the pre-hardened MO–CDP cement and md-AC with 50 wt% MO–CDP were characterized by XRD as shown in Fig. 2. We found that the pre-hardened MO–CDP cement (Fig. 2a) was an apatite structure, which had the characteristic peaks at 26, 30, 32, 33, 34, 40, 46, and 49°, and no additional phase was identified within detectable limits. On the other hand, the phase compositions of the md-AC (Fig. 2b) also clearly showed that an apatite structure with the characteristic peaks was very similar to those of MO–CDP cement. The results suggested that the md-AC contained a mixture of calcium apatite and magnesium substituted calcium apatite. The presence of calcium apatite [$Ca_{10}(PO_4)_6{\cdot}(OH)_2$] was due to the hydrated reaction of HAC, and magnesium substituted calcium apatite could be attributed to the acidic-basic neutralized reaction of MO–CDP cement containing MgO and $Ca(H_2PO_4)_2{\cdot}H_2O$.

3.4 Degradability of md-AC

Figure 3 shows the weight loss ratio of md-AC with different MO–CDP amounts immersed in Tris–HCl solution as a function of time. Clearly, the md-AC could dissolve in Tris–HCl solution with time, and weight loss ratio increased with the increase of MO–CDP amounts in md-AC. 8.3 and 57.5 wt% of weight loss ratio could reach for md-AC with 0 w% (HAC) and 50 wt% MO–CDP after immersion for 12 weeks, respectively. The results showed that the degradation rate of md-AC with 50 wt% MO–CDP was significantly faster than HAC.

3.5 Formation apatite in SBF

Figure 4 shows the SEM images of the surface morphology of md-AC before and after immersion in SBF for 7 days. The obvious difference of the surface morphology of md-AC was observed before and after immersion in SBF, indicating that the new apatite deposit layer formed on the

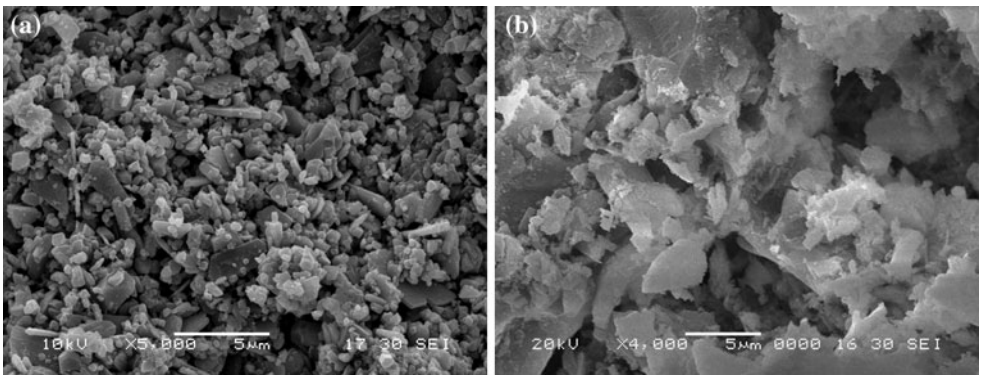

Fig. 1 SEM images of morphology/microstructure of **a** md-AC with 50 wt% MO–CDP and **b** HAC after setting for 48 h

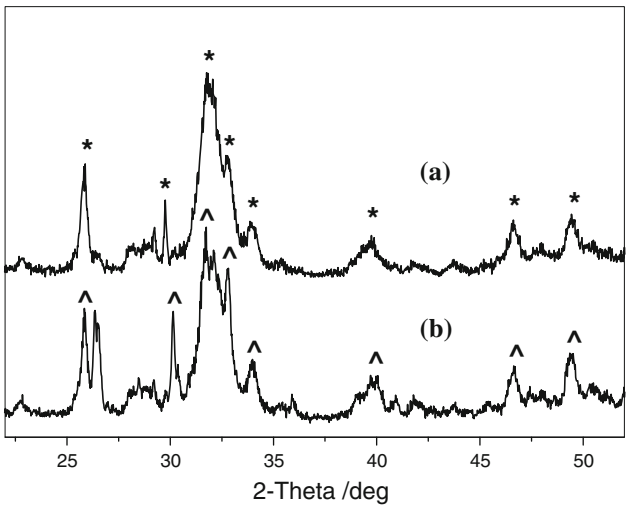

Fig. 2 XRD pattern of **a** MO–CDP cement and **b** md-AC with 50 wt% MO–CDP after setting for 48 h, * represents apatite structure in MO–CDP cement, and ^ represents apatite structure in md-AC cement

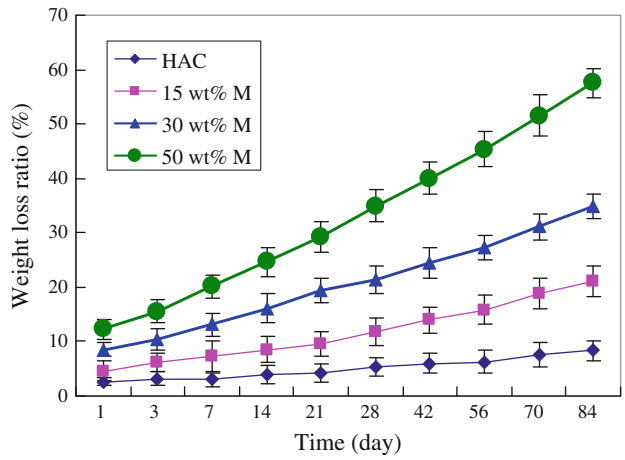

Fig. 3 Weight loss ratio of md-AC with 0, 15, 30, 50 wt% MO–CDP after immersing in Tris–HCl solution over time, data represent the mean ± standard deviation, $n = 3$

md-AC surface. We found that the surface of md-AC included crystal-like small grains while the md-AC surface showed newly flake-like crystals deposit layer that was fully formed on the md-AC surface after immersion in SBF.

Figure 5 shows the changes of ion concentration of Ca, Mg, and P in SBF solution after md-AC with 50 wt% MO–CDP being soaked for various time periods. The ion concentrations of Ca, Mg, and P in SBF solution increased over time, indicating that the dissolution of md-AC had occurred. Figure 5 also shows the changes of pH value of the SBF solution after md-AC immersion for different time periods. The results revealed that the pH of SBF solution varied from 7.5 to 7.25 up to 24 h, and thereafter it changed slightly from 7.25 to 7.3 up to 168 h. The results revealed no obvious changes of pH during soaking.

3.6 Cell proliferation

The proliferation of MG_{63} cells cultured on md-AC with 50 wt% MO–CDP and HAC (as a control) was assessed using MTT assay because optical density (O.D.) values can provide an indicator of the cell growth and proliferation. Figure 6 shows that the O.D. value for md-AC was significantly higher than HAC on days 4 and 7 ($P < 0.05$), no significant difference was found on day 1 for both HAC and md-AC. The results showed that the md-AC could promote the cell proliferation as compared with HAC on days 4 and 7. Thus, the md-AC was biocompatible, with no obvious negative effects on cell growth.

3.7 Cell morphology

Figure 7 shows SEM images of MG_{63} cells cultured on md-AC with 50 wt% MO–CDP for 7 days. The cells firmly attached and spread well on the coarse surface of md-AC, and exhibited normal morphology, indicating that the md-AC had no negative effects on cell morphology and viability. High-magnification SEM images in Fig. 7b further revealed that the coarsely dense layer on md-AC surface consisted of many flake-like crystals, which was similar to the morphology of the md-AC surface after soaked in SBF for 7 days. These results indicated that

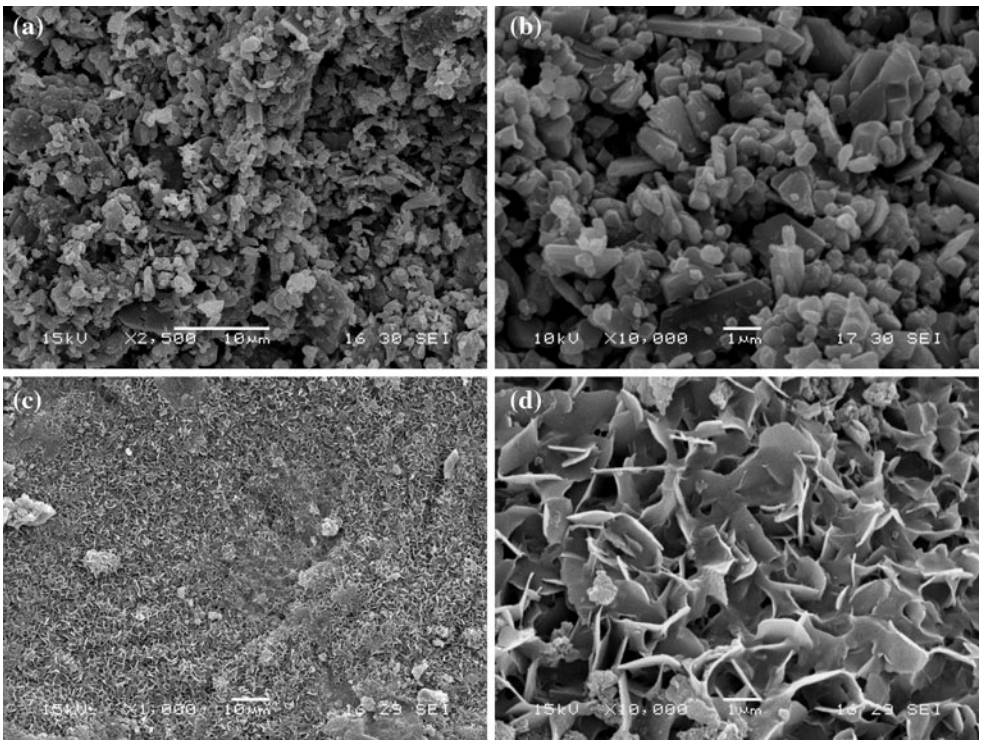

Fig. 4 SEM images of the surface morphology of md-AC with 50 wt% MO–CDP **a**, **b** before and **c**, **d** after immersion in SBF for 7 days

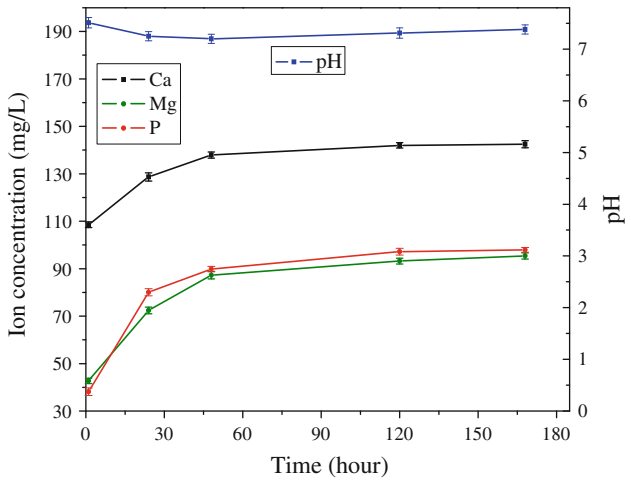

Fig. 5 Change of pH and ion concentration in SBF solution after md-AC with 50 wt% MO–CDP immersing for 7 days, data represent the mean ± standard deviation, $n = 3$

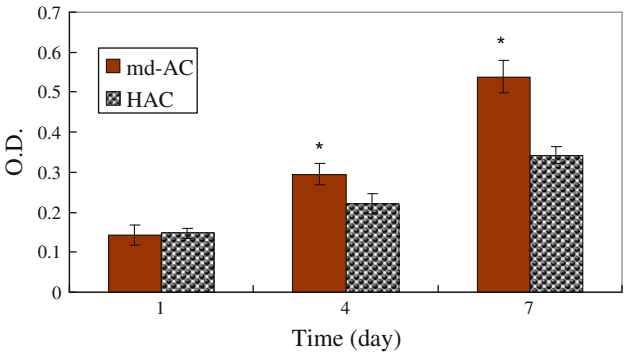

Fig. 6 Cell proliferation on md-AC with 50 wt% MO–CDP and HAC over time, data represent the mean ± standard deviation, $n = 5$

new apatite layer could form on the md-AC surface in cell cultured medium, which facilitated cell spread and growth.

3.8 Cell differentiation

ALP activity assay is generally used to study biochemical markers for expression of osteoblast activity. In this study, cellular differentiation was assessed by testing the ALP activity of MG_{63} cells cultured on md-AC with 50 w% MO–CDP and HAC on 4 and 7 days as shown in Fig. 8. The ALP activity of MG_{63} cells cultured on the md-AC was significantly higher than HAC on 7 days ($P < 0.05$), and there was no significant difference on 4 days for both samples. Thus, the osteoblasts had differentiated better on the md-AC than HAC on 7 days.

4 Discussions

The setting time and compression strength are very important for bone cement biomaterials. In this study, we fabricated the rapid-setting and highly initial mechanical strength of md-AC by adding the mixed powders (MO–CDP)

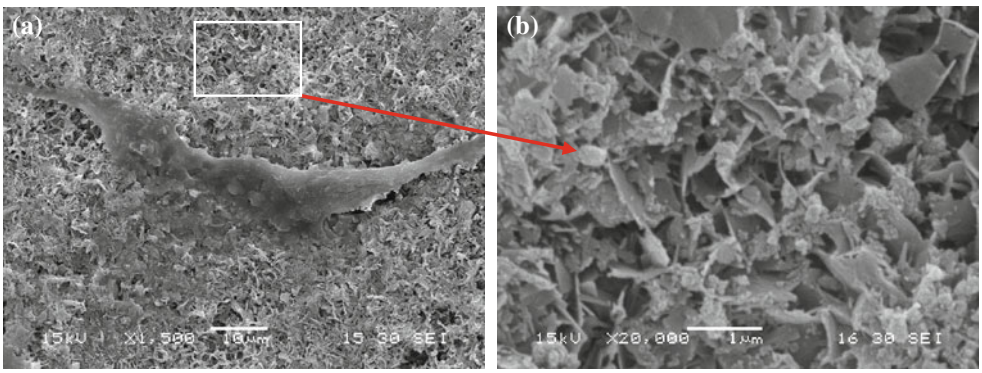

Fig. 7 SEM images of cells cultured on the surface of md-AC with 50 wt% MO–CDP for 7 days

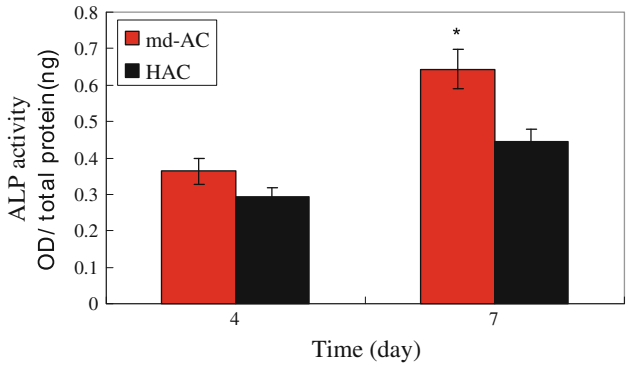

Fig. 8 ALP activity of cells cultured on the md-AC with 50 wt% MO–CDP and HAC at 4 and 7 days, data represent the mean ± standard deviation, $n = 4$

containing $Ca(H_2PO_4)_2{\cdot}H_2O$ and MgO into TECP/DCPA system hydroxyapatite bone cement. The md-AC powders mixed with cement liquid (water) could be easily handled as paste and easily shaped, which can be used as fillers for irregular bone cavity. Our results showed that the setting time of md-AC reduced with the increase of MO–CDP amount, and the optimum setting time of md-AC with 50 wt% MO–CDP was obtained about 6 min, indicating that the md-AC with a fast-setting property had much shorter setting time than HAC. Fast setting is desirable because a long setting time can result in the crumbling of the inserted paste in vivo when it early contacts with physiological fluids.

Bone cements should not only have the characteristics of rapid setting but also adequate mechanical performance that confers immediate load bearing capacity. We found that the initial compression strength of md-AC 50 wt% MO–CDP could reach 51 MPa while that HAC was only 13 MPa after setting for 1 h. Furthermore, after 2 days of setting, the compression strength of md-AC could retain as high as 72 MPa while that of HAC was 38 MPa. The results indicated that the md-AC had highly initial mechanical strength because of the addition of MO–CDP into HAC. The results suggested that the md-AC with good mechanical properties could be used for load-bearing bone repair in some clinic cases.

The morphology/microstructure of md-AC consisting calcium apatite and magnesium substituted apatite was found to form crystal-like small grains, and no obvious difference was observed for the two kinds of apatite crystals in md-AC. There were few cracks on the surface of md-AC, and the apatite crystals were closely combined with together that might provide the mechanical strength for the md-AC hardened body. The pre-hardened md-AC consisted of a mixture of calcium apatite and magnesium substitute apatite demonstrated by XRD. The presence of calcium apatite ($Ca_{10}(PO_4)_6(OH)_2$) was due to the hydration of HAC, and the appearance of magnesium substitute apatite could be attributed to the acid-basic neutralized reaction of magnesium oxide and calcium dihydrogen phosphate. With MgO and $Ca(H_2PO_4)_2{\cdot}H_2O$ in a molar ratio of 7:3, the final product of the MO–CDP cement was $(Mg_3Ca_7)(PO_4)_6(OH)_2$.

The biomaterials used for bone regeneration should be degraded and gradually replaced by newly formed bone tissue in vivo [17]. However, the previous studies have shown that the degradability of the TECP/DCPA system HAC is slow both in vivo and in vitro, and the hydroxyapatite formed by the hydration of HAC has a relatively low dissolution rate, leading to the slow degradation of HAC [2]. Our results revealed that the degradation rate of the md-AC increased with the increase of the MO–CDP amounts in Tris–HCl solution, and the weight loss ratio of the md-AC with 50 wt% MO–CDP and HAC were separately 57.5 and 8.3 wt% after immersion for 12 weeks, indicating that the md-AC had a good dissolubility. The rapid degradation of the md-AC was mainly attributed to its chemical composition, which consisted of $Ca_{10}(PO_4)_6(OH)_2$ and $(Mg_3Ca_7)(PO_4)_6(OH)_2$. Clearly, the degradation of md-AC was accelerated due to the presence of magnesium substitute apatite that had high dissolution compared with HAC.

A common feature of bioactive materials is that they can bond to living bone through new apatite layer that formed on their surfaces in contact with body fluid [18]. Apatite plays an essential role in the formation, growth, and maintenance of the tissue-biomaterial interface [19]. In this

study, we found that newly flake-like apatite could form on the md-AC surface after soaking in SBF for 7 days. The mechanism of newly flake-like apatite formation on the md-AC in SBF was as follows: the md-AC surface provided a favorable site for apatite nucleation, and the release of Ca, Mg and P ions from md-AC increased the ionic activity product of apatite in SBF, thereby promoting the nucleation of apatite and finally resulting in newly flake-like apatite formation on the md-AC surface through a dissolution-deposit process. Thus, apatite layer may provide a suitable substrate for osteoblast-like cell attachment, proliferation, which would form a strong bond between the implanted material and the surrounding bone tissue [20]. Loty et al. found that a biological apatite layer on A-W glass–ceramic promoted osteoblast-like cells differentiation and subsequent apposition of bone matrix in rats [21].

Ideally bioactive biomaterials need to interact actively with cells and stimulate cell growth [22]. In this study, the results showed that the MG_{63} cells could proliferate on the md-AC, as demonstrated by the MTT assay. Furthermore, the proliferation ratio on the md-AC was obviously higher than that on HAC, indicating that the md-AC promoted cellular proliferation superior to HAC. Thus, the md-AC was cytocompatible, with no obvious negative effects on cellular viability. Besides proliferation, the ability of steoblasts differentiation on the biomaterials indirectly reveals that the biomaterials are biocompatible [23]. ALP activity has been used as an early marker for functionality and differentiation of osteoblasts in vitro experiments [24]. In this study, the ALP activity of the MG_{63} cells on the md-AC exhibited significantly higher levels of expression than HAC on day 7, indicating that the cells on md-AC differentiated more quickly than those at HAC.

Cellular responses to a biomaterial, such as proliferation and differentiation, not only depend on its surface morphology but also chemical composition [25]. Because the chemical compositions play crucial roles in determining cell behaviors, they influence the quantity of ions release from the biomaterial and the consequent cell-material interaction [26]. Previous studies have confirmed that the ion dissolution products containing Ca and Mg from bioactive glasses and ceramics can stimulate osteoblast proliferation and differentiation [27–30]. The release of magnesium ions from corroding magnesium alloys should not cause toxicity (local or systemic), and may even have beneficial effects on cell responses in the relevant local tissues [31]. In this study, Mg and Ca ions could be released from the md-AC into SBF solution. Moreover, MTT assay showed that the md-AC had obviously stimulated MG_{63} osteoblast-like cell proliferation on days 4 and 7, and ALP tests revealed that the md-AC exhibited significantly increased cell differentiation on day 7. This increased cell responses probably resulted from the release of Mg and Ca ions from md-AC, and the continuous dissolution associated with the md-AC produced a calcium- and Mg-rich environment that may be responsible for stimulating cell proliferation and differentiation.

The biocompatibility is very closely related to the cell behavior in contact with the bioactive biomaterials and particularly to cell spread on their surface [32]. A recent study shows that the surface of the bioactive materials influences the behavior and morphology of osteoblasts cultured on its surface [33, 34]. In our study, the SEM results revealed that the cells spread well and intimately attached to the md-AC surface on day 7, indicating that the md-AC had no negative effects on cell morphology and viability. The results also showed that the new apatite layer could form on the md-AC surface in cell cultured medium, which may facilitate cell spread and growth. This result indicated that the md-AC had good bioactive surface favorable for cell adhesion and growth and has a good biocompatibility.

5 Conclusions

We fabricated magnesium doped apatite biocement, which could be easily handled as paste that could harden within 6 min, and achieve the compression strength of 51 MPa after setting for 1 h. The finally hardened products of md-AC were mainly $(Mg_3Ca_7)(PO_4)_2(OH)_2$ and $Ca_{10}(PO_4)_2(OH)_2$, and the degradability of the md-AC in Tris–HCl solution significantly increased with the increase of MO–CDP amount. The md-AC had a good bioactivity because apatite could deposit on its surface after soaked in SBF for 7 days. The cell proliferation of MG_{63} cells on md-AC significantly improved compared with HAC, and the ALP activity of MG_{63} cells on the md-AC expressed obviously higher levels than HAC on day 7. The MG_{63} cells with normal phenotype spread well and attached intimately on the md-AC surface, revealing good biocompatibility. These results suggested that the md-AC had a promising application prospect for bone repair.

Acknowledgments This study was supported by grants from the National Natural Science Foundation of China (No. 30970720), The Project-sponsored by SRF for ROCS, SEM (2008), Nano special program of Science and Technology Development of Shanghai (No. 1052nm06600), Key Medical Program of Science and Technology Development of Shanghai (No.09411954900), and the Major Program of National Natural Science Foundation of China (No. 50732002).

References

1. Brown WE, Chow LC. A new calcium phosphate water setting cement. In: Brown PW, editor. Cements research progress. Westerville, OH: American Ceramic Society; 1986. p. 352–79.

2. Guo DG, Xu KW, Sun HL, Yong H. Physicochemical properties of TTCP/DCPA system cement formed in physiological saline solution and its cytotoxicity. J Biomed Mater Res A. 2006;77: 313–23.
3. Guo H, Su JC, Wei J, Kong H, Liu CS. Biocompatibility and osteogenicity of degradable Ca-deficient hydroxyapatite scaffolds from calcium phosphate cement for bone tissue engineering. Acta Biomater. 2009;5:268–78.
4. Arise RO, Davies FF, Malomo SO. Independent and interactive effect of Mg^{2+} and Co^{2+} on some kinetic parameters of rat kidney alkaline phosphatase. Sci Res Ess. 2008;3:488–94.
5. Zreiqat H, Howlett CR, Zannettino A, Evans P, Schulze-Tanzil G, Knabe C, et al. Mechanisms of magnesium-stimulated adhesion of osteoblastic cell to commonly used orthopaedic implants. J Biomed Mater Res. 2002;62:175–84.
6. Revell PA, Damien E, Zhang XS, Evnas P, Howlett CR. The effect of magnesium ions on bone bonding to hydroxyapatite coating on titanium alloy implants. Biocermics. 2004;254: 447–50.
7. Staiger MP, Pietak AM, Huadmai J, Dias G. Magnesium and its alloys as orthopedic biomaterials: a review. Biomaterials. 2006; 27:1728–34.
8. Gu XN, Zheng YF, Cheng Y, Zhong SP, Xi TF. In vitro corrosion and biocompatibility of binary magnesium alloys. Biomaterials. 2009;30:484–98.
9. Huang Y, Jin XG, Zhang XL, Sun HL, Tu JW, Tang TT, Chang J, Dai KR. In vitro and in vivo evaluation of akermanite bioceramics for bone regeneration. Biomaterials. 2009;30:5041–8.
10. Marchi J, Dantas ACS, Greil P, Bressiani JC, Bressiani AHA, Muller FA. Influence of Mg-substitution on the physicochemical properties of calcium phosphate powders. Mater Res Bull. 2007; 42:1040–50.
11. Jia JF, Zhou HJ, Wei J, Jiang X, Hong H, Chen FP, Wei SC, Shin JW, Liu CS. Development of magnesium calcium phosphate biocement for bone regeneration. J R Soc Interf. 2010;7:1171–80.
12. Hofmann MP, Mohammed AR, Perrie Y, Gbureck U, Barralet JE. High-strength resorbable brushite bone cement with controlled drug-releasing capabilities. Acta Biomater. 2009;5:43–9.
13. Liu CS. Inorganic bone adhesion agent and its use in human hard tissue repair. US Patent No.7094286B2.
14. Wu ZZ, Zhang J, Chen TY, Liu CS, Chen ZW. Experimental study of a new type of cement on tibia plateau fractures treatment. Clin Med J China. 2005;12:261–4.
15. Fan Wu, iacan Su, Jie Wei, Han Guo, Changsheng Liu. Self-setting bioactive calcium-magnesium phosphate cement with high strength and degradability for bone regeneration. Acta Biomater. 2008;6:1873–84.
16. Wei J, Jia JF, Wu F, Wei SC, Zhou HJ, Zhang HB, Shin JW, Liu CS. Hierarchically microporous/macroporous scaffold of magnesium-calcium phosphate for bone tissue regeneration. Biomaterials. 2010;31:1260–9.
17. Hench LL, Polak M. Third-generation biomedical materials. Science. 2002;295:1014–7.
18. Zhao WY, Wang JY, Zhai WY, Wang Z, Chang J. The self-setting properties and in vitro bioactivity of tricalcium silicate. Biomaterials. 2005;26:6113–21.
19. Chengtie Wu, Chang Jiang, Siyu Ni, Wang Junying. In vitro bioactivity of akermanite ceramics. J Biomed Mater Res A. 2006;76:73–80.
20. Saboori A, Rabiee M, Mutarzadeh F, Sheikhi M, Tahriri M, Karimi M. Synthesis, characterization and in vitro bioactivity of sol-gel-derived SiO_2–CaO–P_2O_5–MgO bioglass. Mater Sci. 2009;29:335–40.
21. Loty C, Sautier JM, Boulekbache H, Kokubo T, Kim HM, Forest N. In vitro bone formation on a bone-like apatite layer prepared by a biomimetic process on a bioactive glass-ceramic. J Biomed Mater Res. 2000;49:423–34.
22. Sader MS, LeGeros RZ, Soares GA. Human osteoblasts adhesion and proliferation on magnesium-substituted tricalcium phosphate dense tablets. J Mater Sci Mater Med. 2009;20:521–7.
23. Bigi A, Bracci B, Cuisinier F, Elkainm R, Fini M, Mayer I, et al. Human osteoblast response to pulsed laser deposited calcium phosphate coatings. Biomaterials. 2005;26:2381–9.
24. Benoit DSW, Schwartz MP, Durney AR, Anseth KS. Small functional groups for controlled differentiation of hydrogel-encapsulated human mesenchymal stem cells. Nat Mater. 2008; 7:816–23.
25. Qu WJ, Zhong DB, Wu PF, Wang JF, Han B. Sodium fluoride modulates caprine osteoblast proliferation and differentiation. J Bone Miner Metab. 2008;26:328–34.
26. Allen J, Liu Y, Kim YL, Liu Y, Kim YL, Turzhitsky VM, et al. Spectroscopic translation of cell-material interactions. Biomaterials. 2007;28:162–74.
27. Dietrich E, Oudadesse H, Lucas-Girot A, Mami M. In vitro bioactivity of melt-derived glass 46S6 doped with magnesium. J Biomed Mater Res A. 2009;88:1087–96.
28. Sun HL, Wu CT, Dai KR, Chang J, Tang TT. Proliferation and osteoblastic differentiation of human bone marrow-derived stromal cells on akermanite-bioactive ceramics. Biomaterials. 2006; 27:5651–7.
29. Qi GC, Zhang S, Khor KA, Lye SW, Zeng XT, Weng WJ, Liu CM, Venkatraman SS, Ma LL. Osteoblastic cell response on magnesium-incorporated apatite coatings. Appl Surf Sci. 2008; 255:304–7.
30. Feyerabend F, Witte F, Kammal M, Willumeit R. Unphysiologically high magnesium concentrations support chondrocyte proliferation and redifferentiation. Tissue Eng. 2006;12:3545–56.
31. Witte F, Feyerabend F, Maier P, Fischer J, Stormer M, Blawert C, et al. Biodegradable magnesium-hydroxyapatite metal matrix composites. Biomaterials. 2007;28:2163–74.
32. Otsuka M, Oshinbe A, Legeros RZ, Tokudome Y, Ito A, Otsuka K, et al. Efficacy of the injectable calcium phosphate ceramics suspensions containing magnesium, zinc and fluoride on the bone mineral deficiency in ovariectornized rats. J Pharm Sci. 2008;97: 421–32.
33. Lee JY, Kang BS, Hicks B, Chancellor TF, Chu BH, Wang HT, et al. The control of cell adhesion and viability by zinc oxide nanorods. Biomaterials. 2008;29:3743–9.
34. Trimbach DC, Keller B, Bhat R, Zankovych S, Pohlmann R, Schroter S, et al. Enhanced osteoblast adhesion to epoxide-functionalized surfaces. Adv Funct Mater. 2008;18:1723–31.